

HIGHER ORDER FINITE ELEMENT ANALYSIS OF THICK COMPOSITE LAMINATES<sup>1</sup>

J. Goering and H. J. Kim  
 McDonnell Aircraft Company  
 McDonnell Douglas Corporation, St. Louis, MO

## SUMMARY

A higher order, sub-parametric, laminated, 3-D solid finite element has been used for the analysis of very thick laminated composite plates. The geometry of this element is defined by four nodes in the X-Y plane which define a prism of material through the thickness of the laminate. There are twenty-four degrees of freedom at each node; translations at the upper and lower surfaces of the laminate in each of the three coordinate directions, and the derivatives of these translations with respect to each coordinate. This choice of degrees of freedom leads to displacement and strain compatibility at the corners. Stacking sequence effects are accounted for by explicitly integrating the strain energy density through the thickness of the element.

The laminated solid element has been combined with a gap-contact element to analyze thick laminated composite lugs loaded through flexible pins. The resulting model accounts for pin bending effects that produce non-uniform bearing stresses through the thickness of the lug. A thick composite lug experimental test program was performed, and provided data that was used to validate the analytical model. Two lug geometries and three stacking sequences were tested.

## INTRODUCTION

Composite lugs provide a mechanism for the transfer of concentrated loads from one structural member to another. The most notable examples are lugs that transmit wing loads into carry-through bulkheads. The geometry of these lugs can vary substantially for different applications, but they are typically very thick ( $\gg 1$  inch) and may be required to carry out-of-plane as well as in-plane loads. In addition, effects such as pin bending may result in complex stress states through the thickness of the laminate, even when it is only loaded in-plane.

The wide range of variables associated with the design and analysis of thick composite lugs necessitates the use of an analytical model that is adaptable, both in the range of geometries and types of load conditions that can be analyzed. The complex stress distributions that may develop through the thickness require that the model be capable of predicting

<sup>1</sup>The work described in this paper was performed under the NASA ACT contract NAS1-18862, 'Innovative Composite Aircraft Primary Structures.'

three dimensional stress fields. The finite element method is one such method, and is the method that was chosen for this program.

Aircraft components that are fabricated from laminated composites are typically analyzed using plate elements that are based on classical laminated plate theory. These elements are simple to use, since the geometry of the element can be defined in two dimensions, and they account for in-plane and out-of-plane loads. They are of limited use for the analysis of thick lugs, however, since their derivation permits only linear variations in the in-plane stresses through the thickness of the element, and out-of-plane stresses are assumed to be negligible.

At the other extreme, a thick lug can be modeled with three dimensional solid finite elements. Using this approach, each ply can be modeled discretely with one or more elements through the thickness of each ply, or groups of plies can be lumped into a single element. These elements are based on assumed three dimensional displacement fields, and allow complete generality in defining the lug geometry and loads. Although models generated with these elements provide accurate results, their use is cumbersome and they require substantial computing resources. They are therefore not recommended for the type of parametric study that would be required to optimize a lug design. The approach described in this paper is based on a subparametric laminated solid element and represents a compromise between the two methods described above.

#### ANALYTICAL DEVELOPMENT

The thick composite analysis developed for this program uses a subparametric laminated solid element that was developed in [1]. Geometric shape functions for the element are linear in the x-y plane and constant in the z direction, and displacement fields are defined by cubic shape functions in three dimensions. The element geometry is defined by four nodes that specify the (x,y) positions of the edges of a right prism (Figure 1), and displacement degrees of freedom are retained at each of the eight corners of this prism. Twelve degrees of freedom are specified at each corner; the translation in each coordinate direction (3 degrees of freedom), and the partial derivatives of each translation with respect to each coordinate (9 degrees of freedom).

Like conventional homogeneous solid finite elements, the stiffness matrix for the laminated solid element is generated by integrating the strain energy density over the volume of the element. However, the effects of the stacking sequence are included in the laminated solid element by performing the integration numerically over the volume of each ply contained in the element, and summing the result. This process also provides much of the information that will be required in subsequent calculations to determine the strains in each ply.

To account for pin bending effects, both the lug and the pin must be modeled. The generation of these models is relatively simple, since they are explicitly defined in only two dimensions. The through-the-thickness geometry is defined by specifying the ply thickness and stacking

sequence. A typical model is shown in Figure 2. The lug/pin contact is modeled by gap/contact springs that couple lug and pin displacements in the radial direction. The gap/contact springs are bi-linear elements that have a very high stiffness when the gap is closed (the spring is in compression), but zero stiffness when the gap is open (the spring is in tension). Since the extent of the contact area is not known a priori, the analysis must be performed iteratively to determine which gap/contact elements are closed and which are open. The iterative analysis is simplified by treating the lug and pin as substructures which have been reduced such that only degrees of freedom connecting to gap/contact elements are retained. The iterative portion of the analysis is then performed with a model that has only a few dozen degrees of freedom.

The converged solution from the iterative portion of the analysis is used to back substitute for the displacement solution throughout the lug and pin models. The displacement solution is then used to perform a laminate analysis on an element by element basis. For each element, the average strain in a given ply is calculated by integrating the strain field over the volume of that ply in the element, and the average strain in an interface is calculated by integrating over the interface area, as shown in Figure 3. These strains are then used to calculate average stresses in each ply and interface, which are used to perform a failure analysis.

The failure analysis considers three types of failure; 1 - matrix failure within a ply, 2 - fiber failure within a ply, and 3 - failure of an interface. The failure criteria used to assess the failure of a ply is based on Hashin's criteria for a 2-D laminate [2], extended to account for all six stress components. Interfaces are assumed to be isotropic matrix rich regions and failure is assumed to occur when the von Mises stress exceeds the shear allowable for the matrix. Ultimate failure of the laminate is assumed to occur when a fiber failure is predicted for a ply.

## EXPERIMENTAL STUDY

A test program was conducted to investigate the effects of stacking sequence on the strength of thick lugs. The major goal of this study was to determine how stiffness should be distributed through-the-thickness of a laminate to optimize strength. All of the lugs were fabricated from AS4/APC-2, and had the same thickness and external geometry. Combinations of 0,  $\pm 45$ , and 90 degree plies were stacked into four different 30 ply sublaminates, and consolidated in a hydraulic press. Six sublaminates (two each of three different stacking sequences) were combined to form three different 180 ply laminates and co-consolidated in an autoclave. A summary of the lugs tested in this program is shown in Figure 4.

Each laminate contained a similar number of plies in each direction, but their distribution through the thickness was different. This approach produced laminates with equal in-plane properties, but different through-the-thickness stiffness distributions. Two pin sizes were used to investigate different failure modes in the lugs. A 1.00 inch diameter

steel pin was used to generate bearing failures, and a 1.75 inch diameter steel pin was used to generate net section failures. Axial loads were applied to the lugs through the pins by means of a clevis that allowed a .1 inch gap on either side of the lug (Figure 5). A constant gap size (0.1") was maintained throughout the test.

All testing was performed at room temperature with a load rate of 500 lb./sec., and all lugs were tested in as received moisture condition. As expected, the lugs with 1.75 inch diameter holes exhibited a catastrophic fiber failure of the net section, and the lugs with 1.0 inch diameter holes showed permanent yielding around the hole prior to experiencing shear/bearing failures. The initial bearing failure load was determined by observing the behavior of axial strain data from rosettes located 0.5 inch away from the edge of the 1.0 inch hole and 0.25 inch away from the 1.75 inch hole at the center line of specimens. Load-strain data collected during the tests indicated axial strain decreases associated with bearing failure ahead of the 1.0" pin, as shown in Figure 6.

## RESULTS AND DISCUSSION

Models of the test lugs were generated using the laminated solid element. All models used the 2-D mesh shown in Figure 7, which took advantage of the symmetry of the lug to reduce the size of the analytical problem. A convergence study was performed to determine if the through-the-thickness stress distribution in the lug could be predicted using only one element through the thickness. This study showed that the through-the-thickness stress distributions were very complex, and that multiple elements were required to approximate the gradients near the surface of the lug. The results of this study are shown in Figure 8. Four elements were used through the thickness of all subsequent models.

Analysis of the lugs indicated that, for bearing critical lugs (1.00 inch diameter pin), the stacking sequence which placed stiffer material at the center of the lug would be the strongest, and for net section critical lugs (1.75 inch diameter pin), the lug with uniformly distributed stiffness would be strongest. This analytical prediction was confirmed by static tests performed on the lugs. However, the magnitude of the differences in strengths of the various stacking sequences was not as significant as had been predicted. A summary of the analytical and experimental results is shown in Figure 9.

All analytically predicted strengths were within 8% of the experimental values. The largest differences were for the stacking sequences that placed stiffer material near the surfaces of the lug. The analytical models used elements that were of nearly equal thickness, and it may be possible to improve the analytical results by placing fewer plies in the elements near the surface of the lug where the stress gradients are the highest.

In general, the subparametric laminated solid element provides a reasonably accurate means for predicting the complex state of stress in thick laminates. A computer program, based on the use of this element,

has been developed at MCAIR. This program allows an analyst to define the geometry of a thick laminate in only two dimensions, even when there is more than one element through the thickness. Although they were not important to the studies performed in this program, the laminated solid element includes out-of-plane degrees of freedom, which will allow the element to be used to study lugs that are loaded both in and out of plane.

#### CONCLUDING REMARKS

The objective of this study was pursued through parallel efforts in finite element model development and structural testing of thick thermoplastic composite lugs. The analysis of these lugs in conjunction with the experimental results support the following conclusions.

- An accurate means of predicting the complex state of stress in thick composites has been demonstrated through the use of the higher order finite element formulation.
- Caution should be used in the modeling and analysis of thick composite sections since multiple elements may be required through-the-thickness even for higher order elements, as demonstrated in the convergence study.
- Accuracy in predicting the pin bending effect is unclear. The deficiencies in failure loads for the different stacking sequences tested were not large enough to make an accurate assessment of pin bending effects possible.

#### REFERENCES

- [1] Goering, J., "Initial Impact Damage of Composites," Final Technical Report for AFWAL Contract FY1457-85-02143, March 1987.
- [2] Hashin, Z., "Failure Criteria for Unidirectional Fiber Composites," Journal of Applied Mechanics, Vol. 47, June 1980.

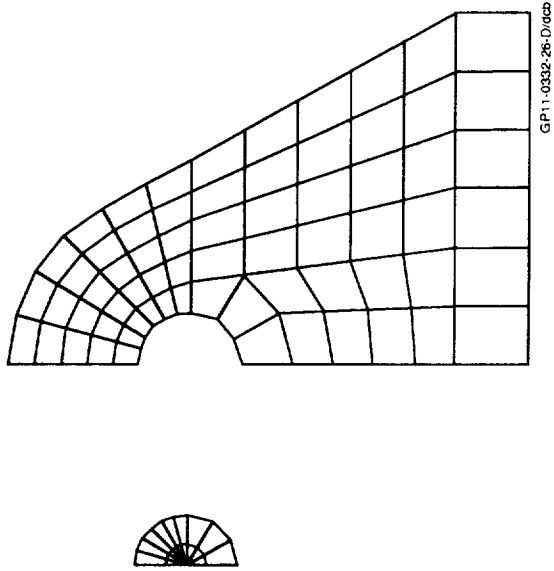


Figure 2. Typical 2-D Lug and Pin Models

GP11-0332-26-D/accb

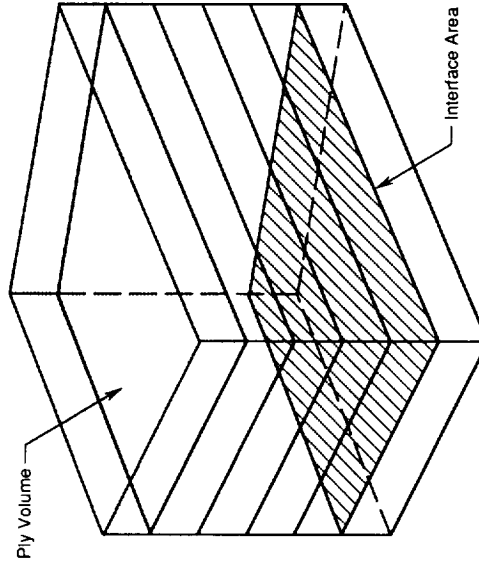


Figure 3. Ply Volumes and Interface Areas With an Element

GP11-0332-20-D/accb

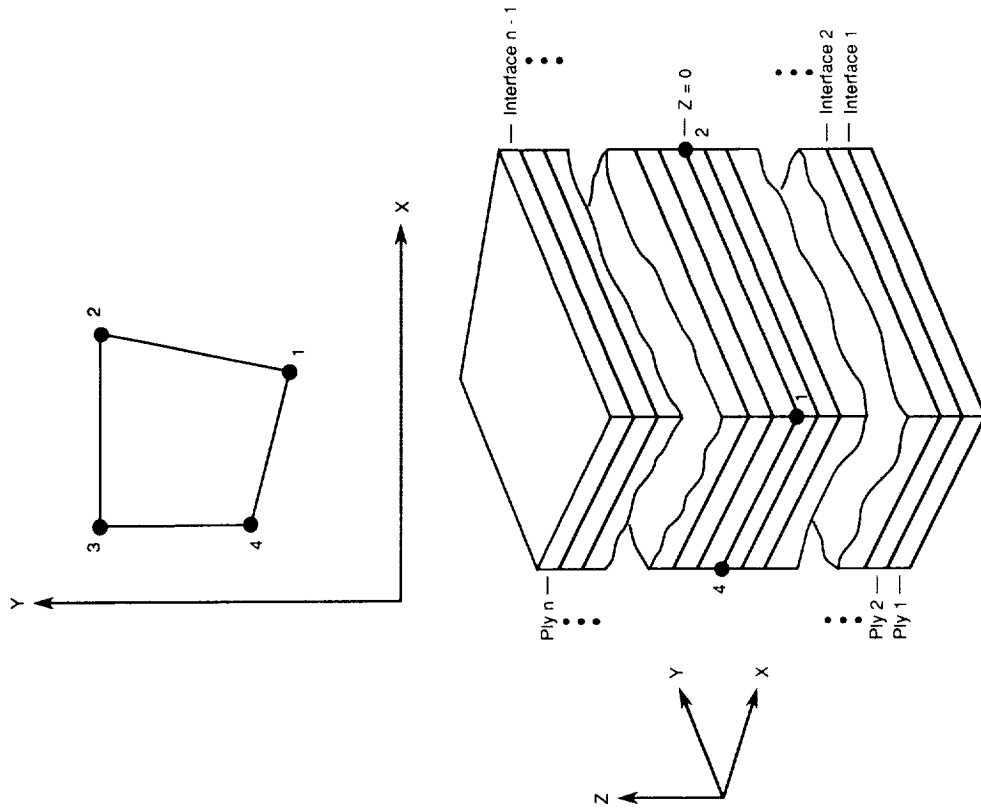
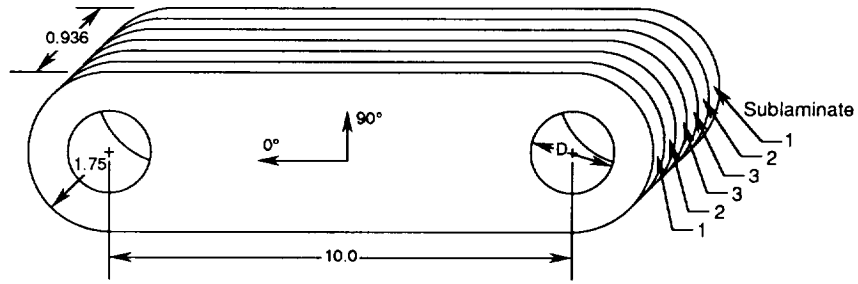


Figure 1. Subparametric Laminated Solid Element

GP11-0332-25-D/accb

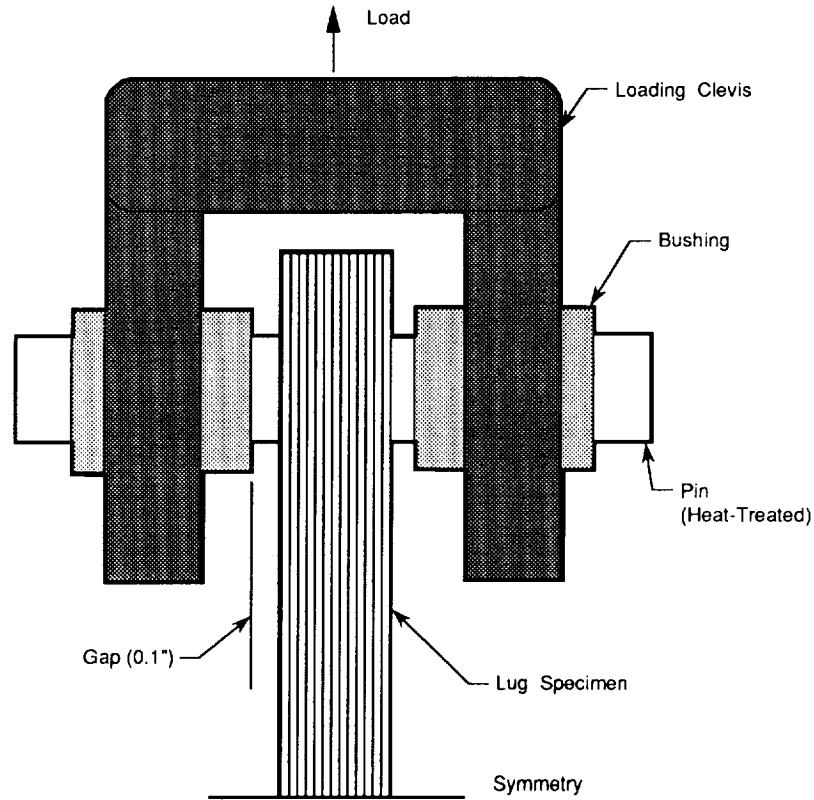


| Lug Specimens | Quantity | Hole Diameter (in.) | Sublaminata Stacking Distribution |               |               |
|---------------|----------|---------------------|-----------------------------------|---------------|---------------|
|               |          |                     | Sublaminata 1                     | Sublaminata 2 | Sublaminata 3 |
| Static 1      | 4        | 1.00                | (47/40/13)                        | (47/40/13)    | (47/40/13)    |
| Static 2      | 3        | 1.00                | (47/40/13)                        | (34/53/13)    | (60/27/13)    |
| Static 3      | 4        | 1.00                | (60/27/13)                        | (47/40/13)    | (20/67/13)    |
| Static 4      | 4        | 1.75                | (47/40/13)                        | (47/40/13)    | (47/40/13)    |
| Static 5      | 4        | 1.75                | (47/40/13)                        | (34/53/13)    | (60/27/13)    |
| Static 6      | 4        | 1.75                | (60/27/13)                        | (47/40/13)    | (20/67/13)    |

\* Sublaminata Stacking Sequences are as follows:  
 (47/40/13): [0<sub>2</sub> /45<sub>2</sub> /90<sub>2</sub> /-45<sub>2</sub> /0<sub>2</sub> /45/0/-45/0<sub>2</sub> ]s  
 (34/53/13): [45<sub>2</sub> /0<sub>2</sub> /-45<sub>2</sub> /90<sub>2</sub> /45<sub>2</sub> /0/-45<sub>2</sub> /0]s  
 (60/27/13): [0<sub>2</sub> /45/0<sub>2</sub> /-45/0<sub>2</sub> /45/0<sub>2</sub> /-45/90<sub>2</sub> /0]s  
 (20/67/13): [45<sub>2</sub> /0/-45<sub>2</sub> /90/45<sub>2</sub> /0/-45<sub>2</sub> /90/45/0/-45]s

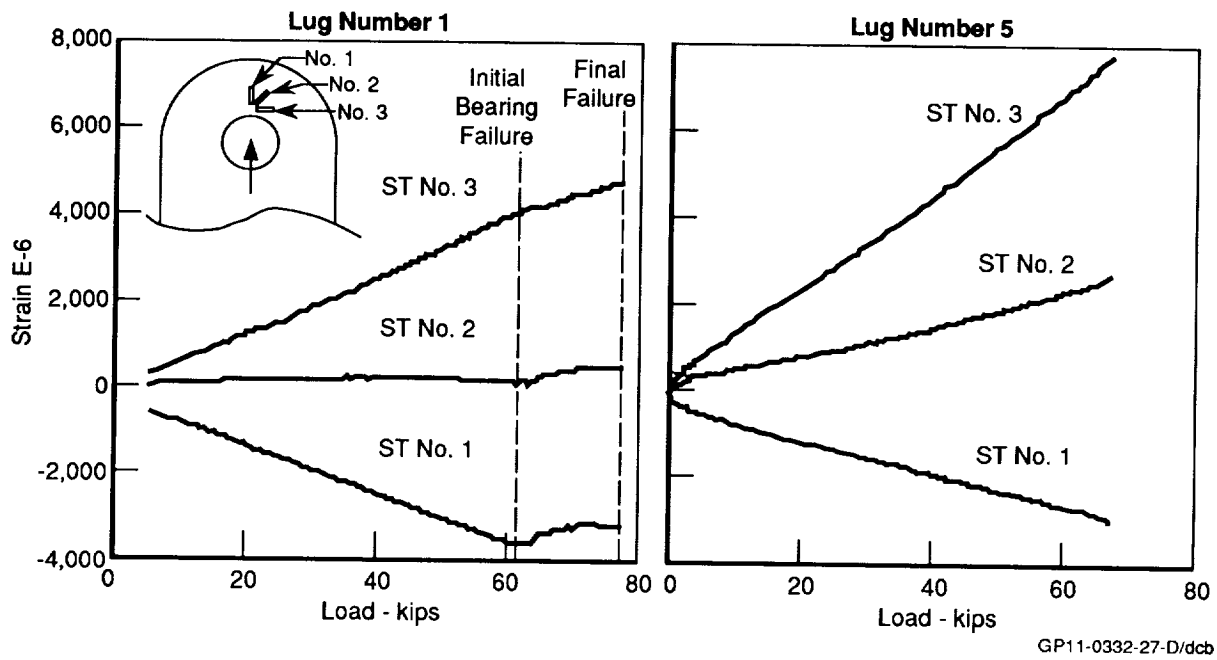
GP11-0332-21-D/s

Figure 4. Configuration and Stacking Sequence of Test Specimens



GP11-0332-28-D/dcb

Figure 5. Test Apparatus



**Figure 6. Load-Strain Curves for Composite Lugs**

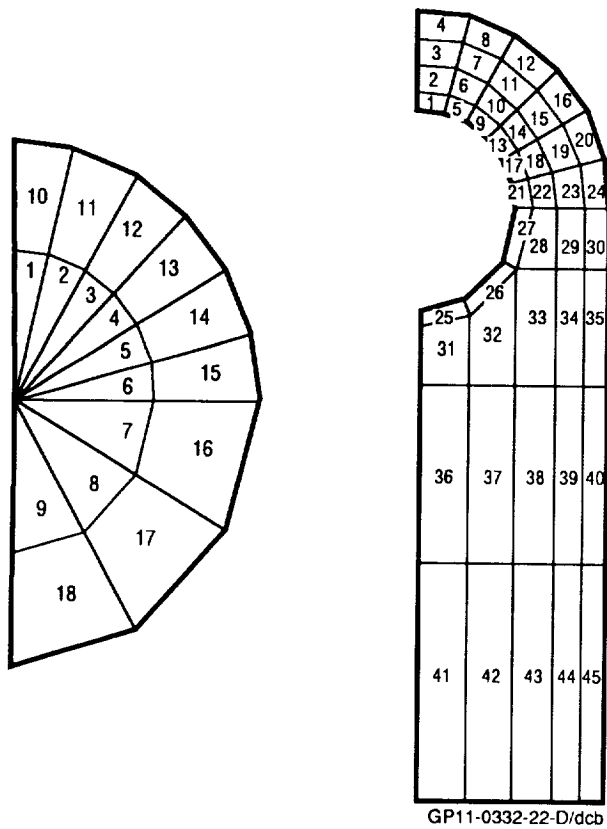


**Figure 7. 2-D Metal for Lug and Pin Models**

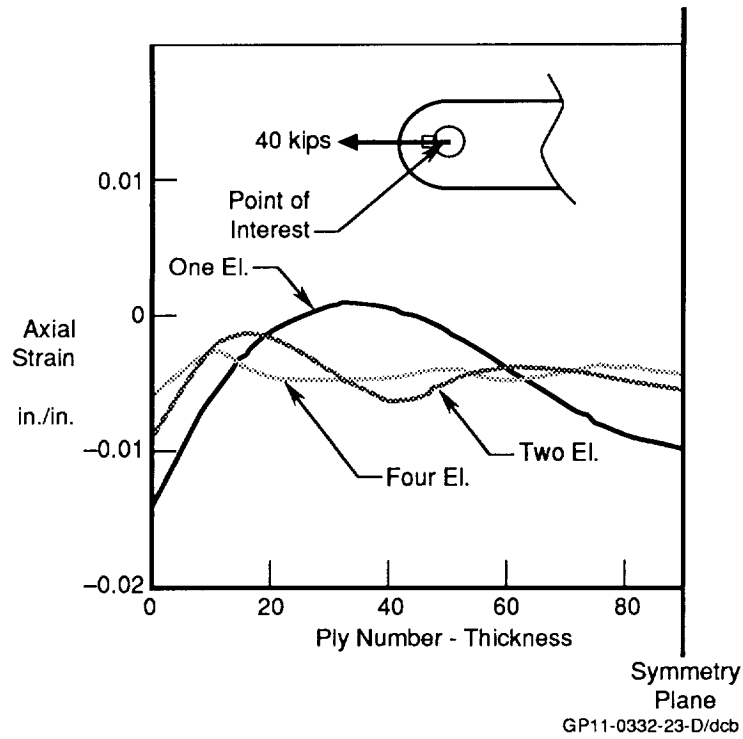


**Figure 8. Convergence Study for Lug Analysis  
(For Lug Type 1)**

| Lug Specimen | Quantity Each | Hole Dia. (in.) | Pred. Failure Load (kips) | Average Test Result (kips) | Standard Deviation |
|--------------|---------------|-----------------|---------------------------|----------------------------|--------------------|
| No. 1        | 4             | 1.00            | 64.2                      | 60.1 (76.7)*               | 4.3 (2.2)          |
| No. 2        | 3             | 1.00            | 65.9                      | 62.3 (74.3)*               | 6.9 (3.0)          |
| No. 3        | 4             | 1.00            | 57.3                      | 62.2 (74.7)*               | 7.0 (2.0)          |
| No. 4        | 4             | 1.75            | 66.9                      | 69.3 **                    | 3.1                |
| No. 5        | 4             | 1.75            | 66.5                      | 68.7 **                    | 2.9                |
| No. 6        | 4             | 1.75            | 61.5                      | 66.8**                     | 1.8.               |

\* Initial Bearing Failure Load (Final Failure Load)

\*\* Failure

GP11-0332-24-D/dcb

**Figure 9. Comparison of Experimental and Analytical Results**

**THIS PAGE INTENTIONALLY BLANK**